

Study of Corrosion and Corrosion Protection of Rebar Steel in Saline Water

Rajesh K. Singh^{1,*}, Vikas Kumar²

Abstract

Corrosion is a major problem with metals. When they come into contact with the surrounding corrosive medium to construct a corrosion cell on their interface, metals undergo corrosion reactions. In such environments, metals can exhibit uniform, galvanic, pitting, stress, crevice, embrittlement, intergranular corrosion, etc. The corrosion phenomenon of rebar steel was studied in saline water. It creates a corrosive medium for rebar steel due to the availability of chloride ions. Rebar steel is used for the construction of bridges, roads, airport, and buildings. These components interact with the saline medium, producing corrosion reactions. Saline water chloride ions attack on rebar steel to form a corrosion cell and corrode metals. Rebar steel is covered with concrete, and the structure is dipped into saline water. By osmosis, chloride ions enter the structure, create dissolving and swelling, chemical corrosion with nonmetallic components, and electrochemical corrosion with metal. For this work synthesized electron rich organic compounds 2-(propan-2-ylidene)propane-1,3-diamine. The corrosion rate of rebar steel was calculated before and after coating by the gravimetric method at different temperatures in the presence of different concentrations of saline water. Potentiostat technique used for the measurement of corrosion potential, corrosion current, and corrosion current density in various concentrations of saline water and coating compound. The surface coverage area and coating efficiency were determined by the corrosion rate of uncoated and coated rebar steel. The coating compound adhered to the surface of the base metal by chemisorption, and confirmed by thermodynamic parameters like activation energy, heat of adsorption, free energy, enthalpy, and entropy. The surface adsorption phenomenon is completed by Langmuir, Freundlich, and Temkin isotherms. The results of thermodynamical parameters and surface adsorption confirmed that the coating compound formed a stable passive barrier, which increased the physical, chemical, and mechanical properties of the rebar steel saline environment.

Keywords: Rebar steel, saline water, coating compound, thermal parameters, surface adsorption, passive barrier

INTRODUCTION

The full corrosion control of materials is a very difficult task, but its effects can be minimized by the application of suitable techniques [1–5]. In a saline water environment, different types of construction activities are going on, like housing, industrialization, various manufacturing, road, railways, bridge, water transport and development of ports for completion. Such work can be completed using metals [6–13]. Cl⁻ ions play a role in chemical and electrochemical reactions with metals and concrete and contribute to the disintegration inside and outside of materials [14–19]. Atmospheric pollutants produce corrosive environments for metallic and nonmetallic substances; thus, corrosion reactions take place in sculptures, monuments, antiques, museums, and living and nonliving species [20–26]. Biometals are used for bone repairing in humans when it comes under

*Author for Correspondence

Rajesh Kumar Singh
E-mail: rks_jpujc@yahoo.co.in

¹Principal, Subject Specialization Chemistry, JLN College, Ghorasahan, East Champaran, Bihar, India.

²Assistant Professor, Department of Chemistry, Government Engineering College, Siwan, Bihar, India.

Received Date: September 30, 2025

Accepted Date: October 24, 2025

Published Date: October 30, 2025

Citation: Rajesh Kumar Singh, Vikas Kumar. Study of Corrosion and Corrosion Protection of Rebar Steel in Saline Water. International Journal of Metallurgy and Alloys. 2025; 11(2): 1–11p.

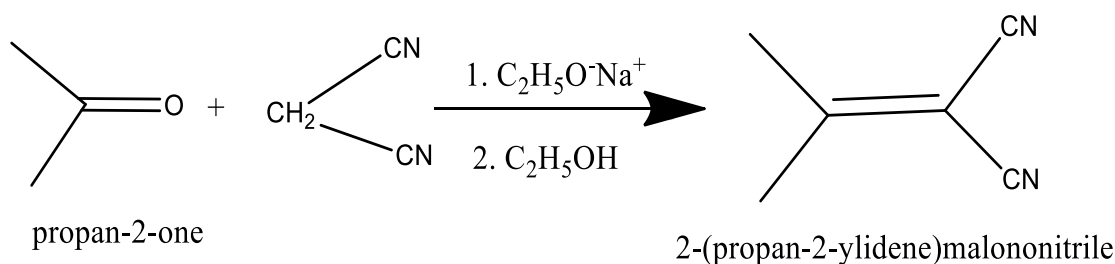
chlorides ions medium to start corrosion reactions. These pollutants corrode building materials as well as tarnish their facial interface. Industrial effluents contain a large amount of acidic [30], which generates a corrosive medium for metals, stones, and cement. Hostile environments are also created by acid rain, global warming, and greenhouse gases. The oxides of carbon, oxides of nitrogen, and oxides of sulfur react with moisture to produce an acidic medium for materials [27–30]. Bio-waste develop microorganisms that release organic acids corrosive medium. Macro-organisms discharge organic acids to form an acidic environment. Corrosion materials are controlled by metallic and nonmetallic coatings, but such coatings do not provide good results in corrosive medium [31–34]. Polymeric and paint coatings mitigate and reduce the corrosion rate of metals. Organic and inorganic inhibitors are used to check the corrosive substances' attack on metals. There are some important coatings applied for corrosion protection materials like electroplating, cladding, spray coating, chemical vapor deposition, structure change, etc. Nanocoating is an important tool of surface protection of metals, but defects of this method are large number of porosities developing on their outer face so corrosive compounds are passed inside materials by the osmosis process and accelerate corrosion reactions. The organic compound 2-(propan-2-ylidene) propane-1,3-diamine can be used to control the corrosion of rebar steel and improve their physical and mechanical properties. It produces good inhibition efficiency and surface coverage area [35–42].

EXPERIMENTAL

Rebar steel is cut into 3cm height and its diameter is 1cm. The outer surface of rubbed with emery paper and washed with acetone to remove dust impurity. The sample immersed into saline water at 3mm, 5mm, 7mm, 9mm, and 11mm concentrations during the mentioned concentrations, temperature required 278, 283, 288, 293, and 298 K. On these parameters, corrosion rates were calculated. The samples were coated with 2-(propan-2-ylidene) propane-1,3-diamine 2 mm, 4 mm, 6 mm, 8 mm, and 10 mm, and their corrosion rate was determined at above-mentioned saline water concentrations and temperatures. The corrosion rate of metal was calculated by the gravimetric method formula $K = 13.56 \times (W_i - W_f) / (D \times A \times t)$ where W_i = initial mass, W_f = final mass, D = density of metal, A = area and t = time. The surface coverage area was determined by the formula $\theta = (K_o - K) / K_o$ where K_o = corrosion rate without coating and K = corrosion rate with coating. The percentage coating efficiency was calculated by formula, $\%CE = (K_o - K) / K_o \times 100$. The surface adsorption phenomenon was determined by the Langmuir isotherm $\log(\theta / (1 - \theta)) = A C e^{-q/RT}$. Activation energy was calculated by formula $K = A e^{-E_a/RT}$. Free energy of coating compound calculated by the formula $-\Delta G = 2.303 R T \log(33.3 K)$. Their enthalpy and entropy were determined by the transition state formula transition formula $K = R T / N h \exp(\Delta S^\ddagger / R) \exp(-\Delta H^\ddagger / R T)$. Stern–Geary equation used to calculate corrosion current $I = \Delta E / \Delta I = \beta_{a1} \times \beta_{c1} / 2.303 I_{o1} (\beta_{a1} + \beta_{c1})$. Corrosion rate of metal was calculated by potentiostat $K_C = (0.1288) \times I \times (E_{eq} / \rho)$.

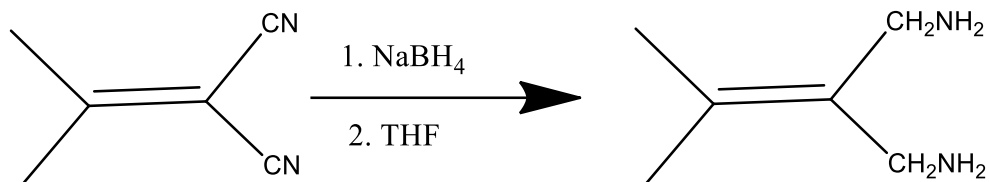
- *Synthesis of 2-(propan-2-ylidene)propane-1,3-diamine:* Propa-2-one added into the solution of methylenedinitrile in the presence of ethyl alcohol and sodium ethoxide to form 2-(propan-2-ylidene)malononitrile.

Scheme 1



- When 2-(propan-2-ylidene)malononitrile is used with sodium borohydride in the presence of THF to produce 2-(propan-2-ylidene)propane-1,3-diamine.

Scheme 2



2-(propan-2-ylidene)malononitrile

2-(propan-2-ylidene)propane-1,3-diamine

RESULTS AND DISCUSSION

Uncoated and coated rebar steel corrosion rates were recorded in Table 1 at different temperatures, concentrations of saline water, and coating compounds. The results of Table 1 indicated that the uncoated rebar steel corrosion rate was found to be high. But it was coated with 2-(propan-2-ylidene)propane-1,3-diamine then the corrosion rate reduced, as trends clearly noticed in Table 1 and Figure 1.

Table 1. Corrosion rates of uncoated and coated rebar steel in saline water.

| Temperature (K) | 278 | 283 | 288 | 293 | 298 |
|----------------------------|---------|---------|--------|---------|---------|
| Concentration (mM) | 2 | 4 | 6 | 8 | 10 |
| Ko | 8912 | 11563 | 11829 | 12324 | 12871 |
| log Ko | 3.949 | 4.063 | 4.072 | 4.091 | 4.095 |
| Ko/T | 32.057 | 35.858 | 39.072 | 44.061 | 47.191 |
| log (Ko/T) | 1.505 | 1.554 | 1.591 | 1.644 | 1.673 |
| K | 1657 | 2337 | 2622 | 3251 | 3685 |
| logK | 3.219 | 3.368 | 3.418 | 3.512 | 3.566 |
| K/T | 5.961 | 8.257 | 9.104 | 11.095 | 12.365 |
| log(K/T) | 0.775 | 0.916 | 0.959 | 1.045 | 1.092 |
| (Ko - K) | 7255 | 9226 | 9207 | 9073 | 9186 |
| $\Theta = (Ko - K/Ko)$ | 0.8141 | 0.7978 | 0.7362 | 0.7136 | 0.7013 |
| %C | 81.41 | 79.78 | 73.62 | 71.36 | 70.13 |
| (1 - θ) | 0.1859 | 0.2022 | 0.2638 | 0.2864 | 0.2987 |
| ($\theta/1 - \theta$) | 4.379 | 4.945 | 2.791 | 2.491 | 2.347 |
| log($\theta/1 - \theta$) | 0.641 | 0.694 | 0.445 | 0.396 | 0.371 |
| Log θ | -0.0893 | -0.0981 | -0.133 | -0.1465 | -0.1541 |
| logC | -2.301 | -2 | -1.824 | -1.699 | -1.602 |

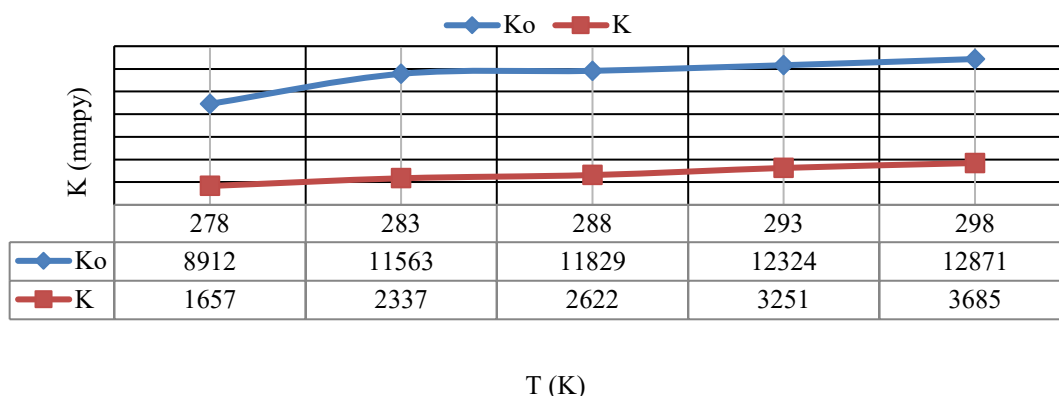


Figure 1. K (mppy) Vs. T (K).

The concentrations of coating compounds increased on the surface of rebar and coated metal dipped into different concentrations of saline water, and their results were depicted in the Table. Such trends were observed in Figure 2.

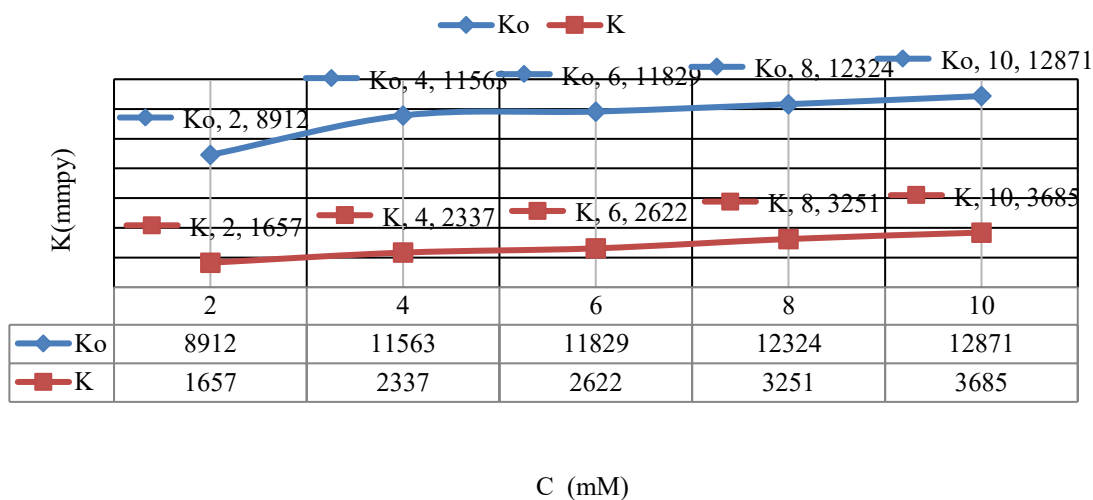


Figure 2. K (mppy) Vs. C (mM).

The results of logKo uncoated rebar steel and logK values coated rebar steel with 2-(propan-2-ylidene) propane-1,3-diamine at different temperatures mentioned in Table 1 and Figure 3. It was observed that the corrosion rate enhanced with uncoated metal after coating, its corrosion rate decreased.

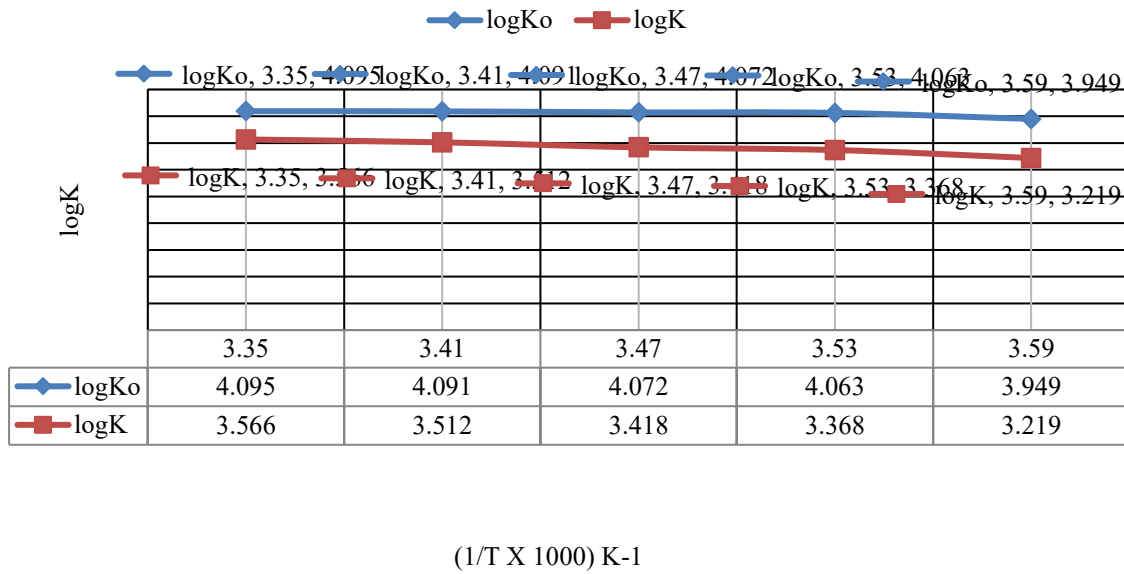


Figure 3. logK Vs. 1/T.

The coating compound 2-(propan-2-ylidene)propane-1,3-diamine $\log(\theta/1 - \theta)$ values at various temperatures are given in Table 1. These results indicated that $\log(\theta/1 - \theta)$ decreased as temperatures increased, as observed in Table 1 and Figure 4.

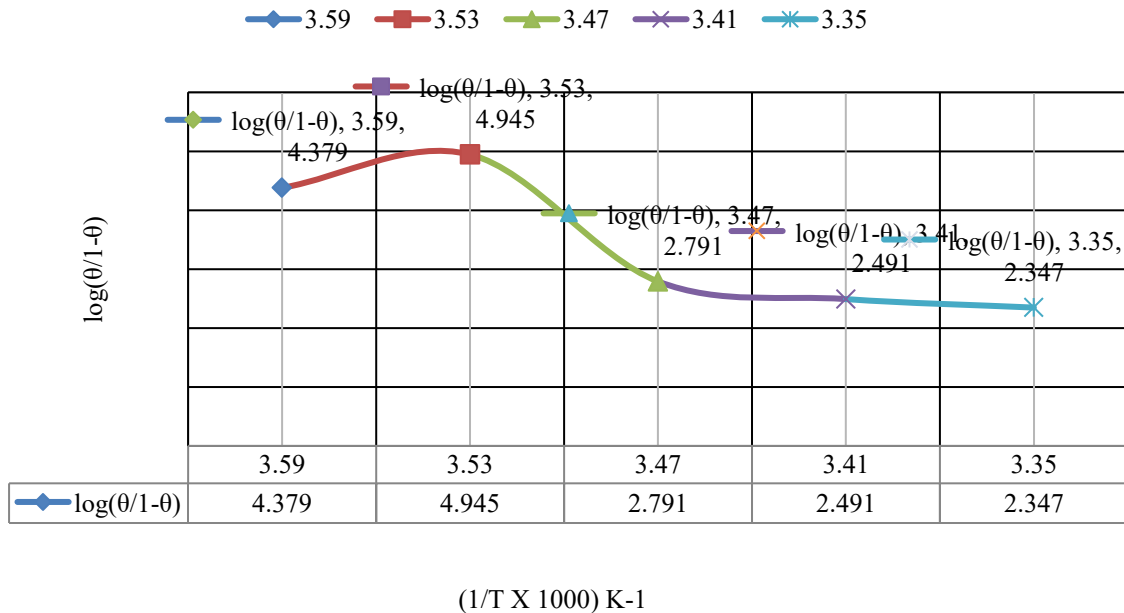


Figure 4. $\log(\theta/1 - \theta)$ Vs. 1/T.

The surface coverage areas occupied by 2-(propan-2-ylidene)propane-1,3-diamine at various temperatures were written in Table 1 and Figure 5. It was observed that at low temperature it covered more surfaces with respect to higher temperature.

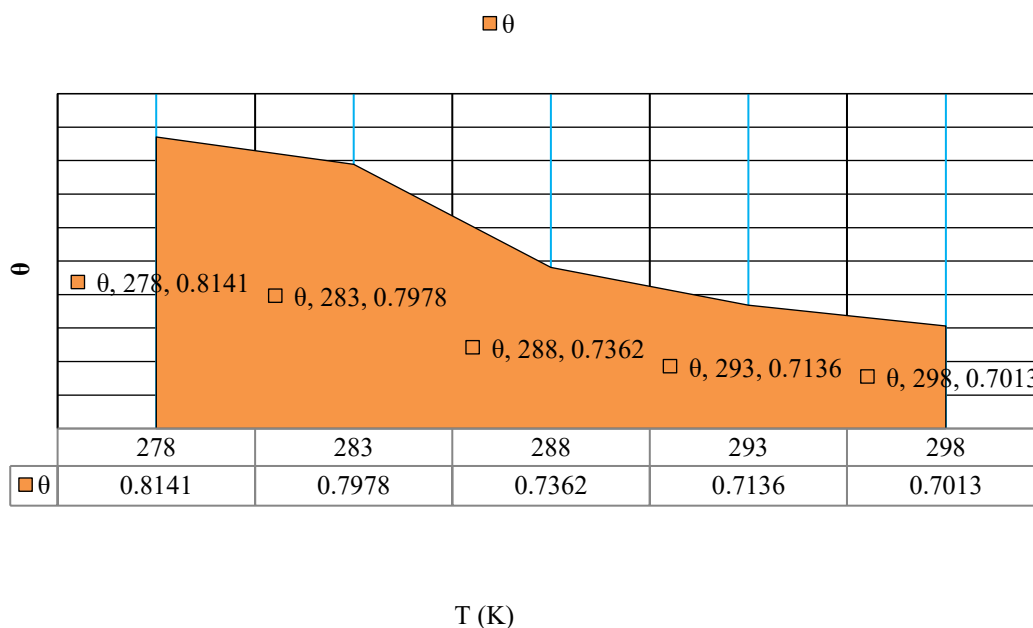


Figure 5. θ Vs. T (K).

The coating efficiencies of 2-(propan-2-ylidene)propane-1,3-diamine were given in Table 1 at different temperatures and Figure 6. These results showed that lower temperature coating efficiencies were found to be as noticeable at higher temperatures.

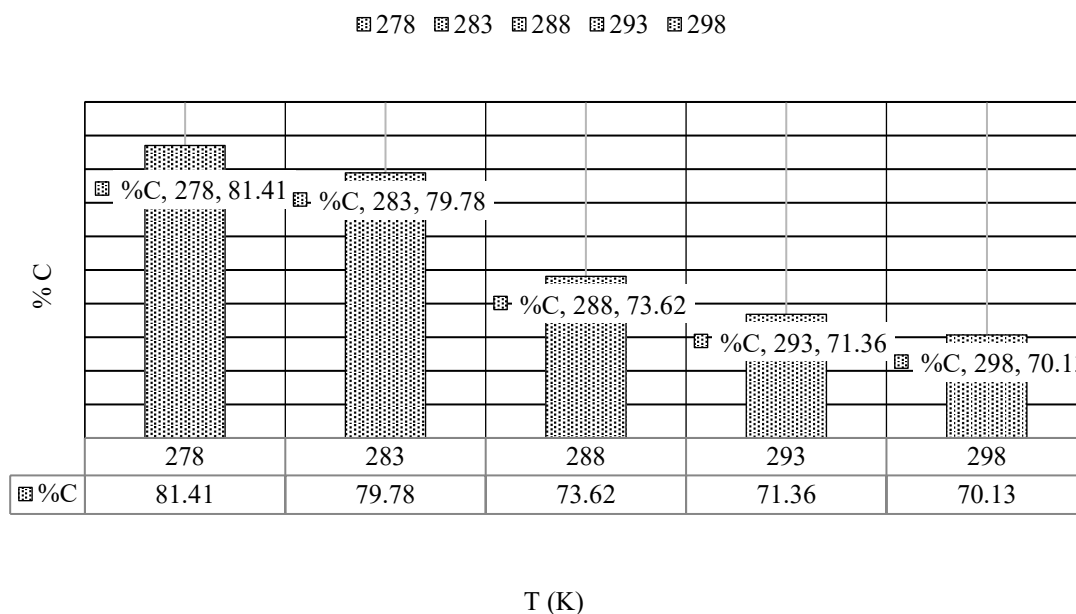


Figure 6. θ Vs T (K).

The plot between $\log \theta$ versus $\log C$ was found to be a straight line, as shown in Figure 7, that line confirms about Freundlich isotherm, so coating compound 2-(propan-2-ylidene)propane-1,3-diamine adsorbed on the base metal surface.

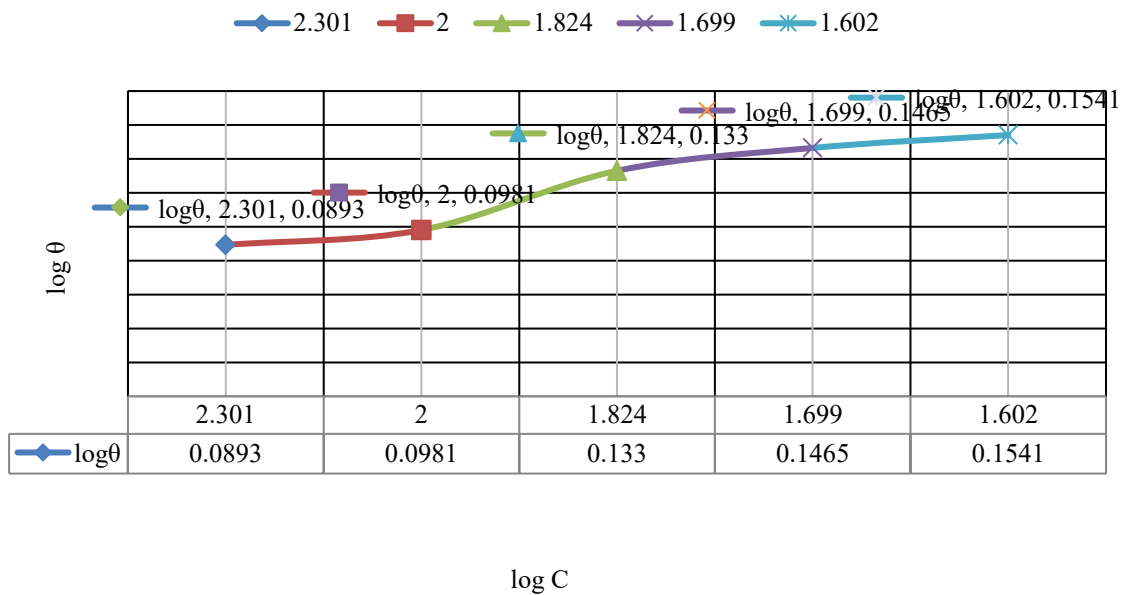


Figure 7. $\log\theta$ Vs $\log C$.

The graph plotted between θ (surface coverage area) versus $\log C$ for the 2-(propan-2-ylidene)propane-1,3-diamine compound produced by a straight line, as noticed in Figure 8, which indicates the Temkin isotherm, so this compound accommodated on rebar steel.

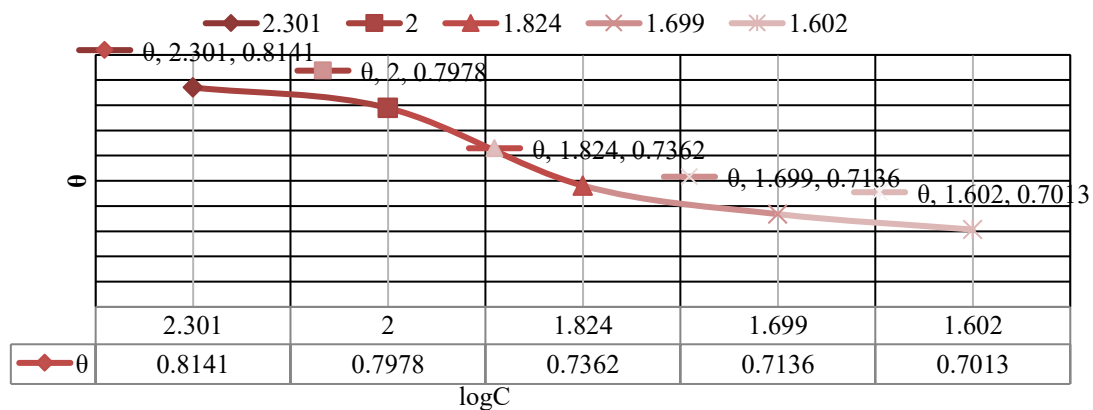


Figure 8. θ Vs. $\log C$.

Figure 9 exhibited the plot between $\log(K/T)$ versus $1/T$ found to be a straight line with help from that graph, calculated enthalpy of 2-(propan-2-ylidene)propane-1,3-diamine.

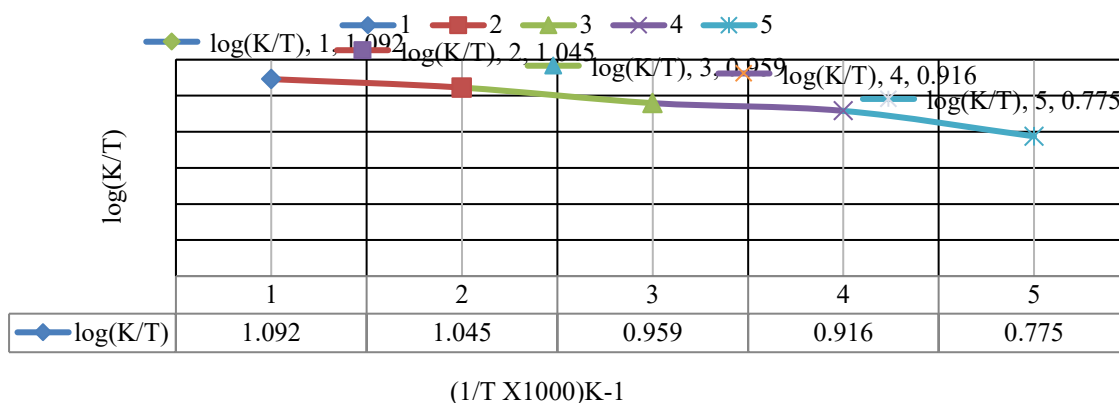


Figure 9. $\log(K/T)$ Vs $1/T$.

The coating compound 2-(propan-2-ylidene)propane-1,3-diamine activation energy, heat of adsorption, free energy, enthalpy, and entropy were calculated in their absence and presence at different temperatures and concentrations in a saline water medium. Their values showed that the coating compound adhered to the rebar steel by chemisorption. Their thermal parameters values decreased after coating, and surface coverage areas increased, as shown in Table 2 and Figure 10.

Table 2. Thermal parameters of 2-(propan-2-ylidene)propane-1,3-diamine.

| Con | 2 mM | 4 mM | 6 mM | 8 mM | 10 mM |
|--------------|-----------|-----------|-----------|-----------|-----------|
| T(K) | 278 | 283 | 288 | 293 | 298 |
| E_0 | 273.7561 | 276.9516 | 272.8472 | 269.3805 | 264.8994 |
| E_1 | 223.1504 | 229.5774 | 229.0255 | 231.255 | 230.6792 |
| Q_1 | -27.10525 | -22.9032 | -21.30781 | -17.44948 | -15.91337 |
| ΔG_1 | -338.5195 | -340.5541 | -338.8208 | -336.629 | -332.1285 |
| ΔH_1 | -53.72525 | -62.4385 | -64.25847 | -68.81022 | -70.63984 |
| ΔS_1 | -148.0204 | -158.9127 | -161.9014 | -167.5284 | -169.7827 |
| θ | 0.8141 | 0.7978 | 0.7362 | 0.7136 | 0.7013 |

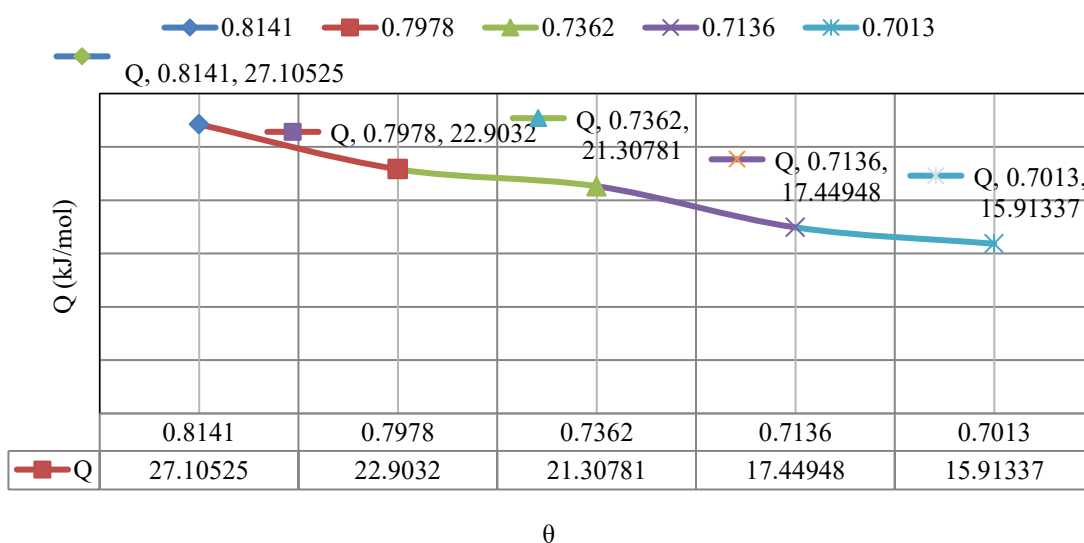


Figure 10. Q Vs $1/T$.

Potentiostatic polarization was used to determine without and with coating electrode potential and corrosion current density, and their results were written in Table 3. It was observed that without coating electrode potential increased, but its values reduced after coating with 2-(propan-2-ylidene)propane-1,3-diamine. The corrosion current enhances without coating, but its value can be decreased after coating, as shown in Figure 11. The corrosion current density increased when rebar steel coated with 2-(propan-2-ylidene)propane-1,3-diamine, as depicted in Table 3 and Figure 11. The corrosion rate obtained by the gravimetric method was matched with the corrosion rate of the potentiostat.

Table 3. Potentiostat polarization results in uncoated and coated rebar steel in saline water.

| | ΔE | ΔI | R_p | i_a | i_c | $i_a \cdot i_c$ | $i_a + i_c$ | $i_a i_c / i_a + i_c$ | $\Delta I / \Delta E$ | I_c | K_{cr} |
|----|------------|------------|-------|-------|-------|-----------------|-------------|-----------------------|-----------------------|-------|----------|
| Co | 950 | 625 | 1.52 | 552 | 401 | 221352 | 953 | 232 | 0.65 | 66 | 281 |
| | 1050 | 725 | 1.44 | 621 | 451 | 280071 | 1072 | 261 | 0.69 | 78 | 332 |
| | 1150 | 925 | 1.24 | 651 | 501 | 326151 | 1152 | 283 | 0.81 | 98 | 419 |
| | 1250 | 1025 | 1.21 | 700 | 552 | 386400 | 1252 | 308 | 0.82 | 109 | 466 |

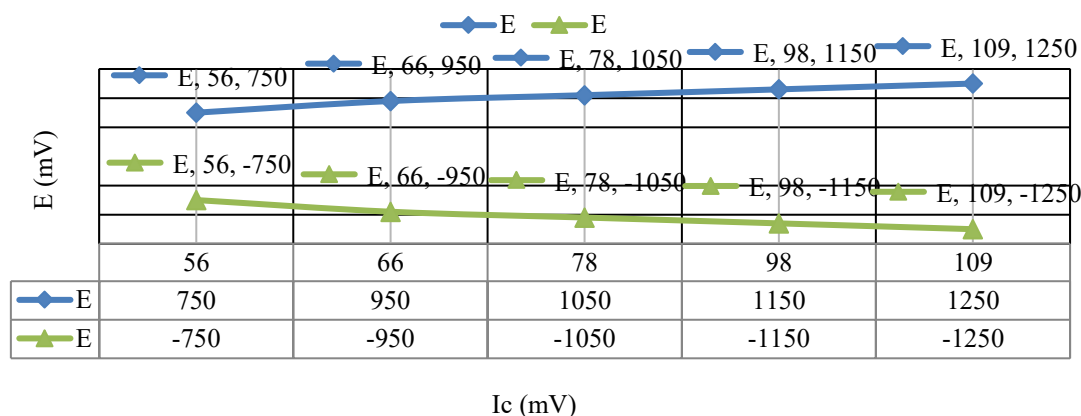
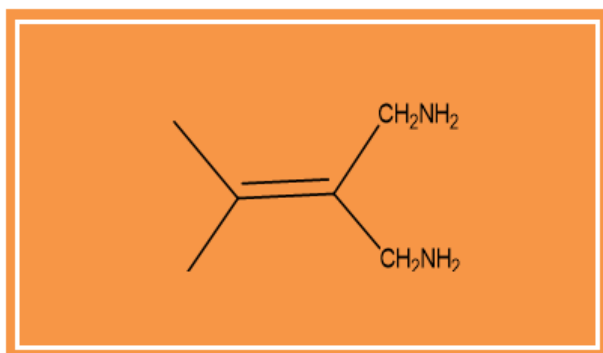


Figure 11. E (mV) Vs. I_c (mA/cm²).

- *Mechanism:* The coating compound 2-(propan-2-ylidene) propane-1,3-diamine is a highly electron-rich substance. It contains two π -electrons and two amino functional groups, so it forms a protective thin film barrier with the base metal, as shown in its structure. This protective barrier checks the attack of chloride ions.



CONCLUSION

The organic compound 2-(propan-2-ylidene)propane-1,3-diamine is used for corrosion mitigation of rebar steel in a saline water medium. This compound's anticorrosive activity was studied at different

temperatures and concentrations. Thermal results showed that 2-(propan-2-ylidene)propane-1,3-diamine formed chemical bonding with the base metal. The protective barrier suppressed the attack of Cl^- ions and its physical, chemical, and mechanical properties saline water environment. Surface adsorption theory, like Langmuir, Freundlich, and Temkin isotherms, confirmed that 2-(propan-2-ylidene)propane-1,3-diamine adsorbed on metal by chemisorption phenomenon. The coating produced good results of efficiency and surface coverage area.

Acknowledgment

The author is thankful to UGC-New Delhi for providing the Major Project, and the title of the Project is Study of Corrosion Protection of the Mahatma Gandhi Setu in Patna, Bihar, India, F. No. 39-707/2010(SR). The author thanks other people who provided data collection and graph plotting.

REFERENCES

1. Condit CW. The reinforced-concrete skyscrapers: The Ingalls Building in Cincinnati and its place in structural history. Technol Cult. 1968.
2. Steiger RW. History of concrete. The Aberdeen Group. 1995.
3. Morgan W. Reinforced concrete. In: Claydon JF, editor. The Elements of Structure. 1995.
4. Department of Civil Engineering. History of concrete building construction. Memphis: University of Memphis; 2015.
5. Collins P. Concrete: The vision of a new architecture. Montreal: McGill-Queen's University Press; 1981. pp. 58–60.
6. Morsch E. Concrete-steel construction (Der Eisenleltobaw). New York: The Engineering News Publishing Company; 1909. pp. 204–205.
7. Kim S, Surek J, Baker-Jarvis J. Electromagnetic metrology on concrete and corrosion. J Res Natl Inst Stand Technol. 2011;116:655–669.
8. Nilson AH, Darwin D, Dolan CW. Design of concrete structures. New York: McGraw-Hill Education; 2003. pp. 80–99.
9. Effect of zinc phosphate chemical conversion coating on corrosion behavior of mild steel in alkaline medium: Protection of rebars in reinforced concrete. Sci Technol Adv Mater. 2008;9:4–9.
10. Birks JW, Calvert JG, Sievers RE. The chemistry of the atmosphere: Its impact on global change—perspectives and recommendations. 1993. p. 170.
11. Brasseur GP, Orlando JJ, Tyndall GS. Atmospheric chemistry and global change. Oxford: Oxford University Press; 1999. p. 654.
12. Davidson O, Metz B. Proceedings of workshop on carbon dioxide capture and storage. Petten: ECN; 2002. p. 106.
13. Feely RA, Sabine CL, Hernandez-Ayon JM, Ianson D, Hales B. Evidence for upwelling of corrosive “acidified” water onto the continental shelf. Science. 2008;320(5882):1490–2. doi: 10.1126/science.1155676.
14. Finlayson-Pitts BJ, Pitts JN. Chemistry of the upper and lower atmosphere. San Diego: Academic Press; 2000. p. 969.
15. Houghton JT, Ding Y, Johnson CA, editors. Climate change 2001. Cambridge: Cambridge University Press; 2001. p. 881.
16. Lamaka SV, Zheludkevich ML, Yasakau KA, Serra R, Poznyak SK, Ferreira MGS. Nanoporous titania interlayer as reservoir of corrosion inhibitors for coatings with self-healing ability. Prog Org Coat. 2007;58(2–3):127–135. doi: 10.1016/j.porgcoat.2006.08.029.
17. Manahan SE. Fundamentals of environmental chemistry. New York: John Wiley & Sons; 2000. p. 268.
18. Maruthamuthu S, Muthukumar N. Role of air microbes on atmospheric corrosion. Curr Sci. 2008;94(3):359–363.
19. Melchers RE, Li CQ. Phenomenological modeling of reinforcement corrosion in marine environments. ACI Mater J. 2006;103(1):25–32.
20. Natesan M, Venkatachari G, Palaniswamy N. Kinetics of atmospheric corrosion of mild steel, zinc, galvanized iron and aluminium at 10 exposure stations in India. Corros Sci. 2006;48(11):3584–3608. doi: 10.1016/j.corsci.2006.02.006.

21. Ohtsu M, Tomoda Y. Acoustic emission techniques for rebar corrosion in reinforced concrete. *Adv Constr Mater*. 2007;7:615–622.
22. Prakash D, Singh RK. Protection of mild steel by thiourea derivative as inhibitors in 20% HCl. *Bull Electrochem*. 2006;22(6):257–261.
23. Prakash D, Singh RK. Protection of stainless steel in 20% HCl by use of organic inhibitors. *J Indian Chem Soc*. 2006;83(12):1256–1259.
24. Prakash D, Singh RK. Corrosion inhibition of mild steel in 20% HCl by some organic compounds. *Indian J Chem Technol*. 2006;13:555–560.
25. Quinet M, Neveu B, Moutarlier V, Audebert P, Ricq L. Corrosion protection of sol–gel coatings doped with an organic corrosion inhibitor: Chloranil. *Prog Org Coat*. 2007;58(1):46–53. doi: 10.1016/j.porgcoat.2006.11.007.
26. Shi HW. Corrosion protection of AZ91D magnesium alloy with sol-gel coating containing 2-methyl piperidine. *Prog Org Coat*. 2009;66(3):183–191. doi: 10.1016/j.porgcoat.2009.07.004.
27. Singh RK. Comparative study of mild steel and stainless steel inhibition in 20% HCl solution by some organic inhibitors. *Bull Electrochem*. 2007;23:113–117.
28. Singh RK. Comparative study of the corrosion inhibition of mild steel and stainless steel by use of thiourea derivatives in 20% HCl solution. *J Metall Mater Sci*. 2009;51:225–232.
29. Singh RK. Corrosion protection of stainless steel in oil well recovery. *Mater Sci Res India*. 2009;6(2):459–466. doi: 10.13005/msri/060225.
30. Singh RK. The Corrosion Protection of Stainless Steel in Phosphate Industry. *J Metall Mater Sci*. 2010;52:173–180.
31. Singh RK. The corrosion protection of materials by nanotechnology. *Mater Sci Res India*. 2011;8:353–355. doi: 10.13005/msri/080224.
32. Singh RK. Corrosion control techniques for existing and new marine infrastructure. *Masterbuilder*. 2015;17:56–58.
33. Singh RK. Building materials corrosion by fiber reinforced polymers. *Powder Metall Min*. 2015;1:1–5. doi: 10.4172/2168-9806.1000137.
34. Singh RK, Kumar R. Study corrosion and corrosion protection of stainless steel in phosphate fertilizer industry. *Am J Min Metall*. 2014;2(2):27–31. doi: 10.12691/ajmm-2-2-2.
35. Singh RK, Prakash D. Inhibition of stainless steel by use of thiourea derivative as inhibitors in 20% HCl. *J Indian Chem Soc*. 2008;85(6):643–646.
36. Singh RK, Thakur MK, Latif S. Corrosion protection of building materials in marine environment by nanocoating and filler techniques. *Masterbuilder*. 2018;20:68–76.
37. US Environmental Protection Agency (EPA). Greenhouse gases and global warming potential values. In: *Inventory of US Greenhouse Emissions and Sinks: 1990–2000*. Washington (DC): US EPA; 2002. p. 16.
38. Vishwanadh B, Balasubramaniam R, Srivastava D, Dey GK. Effect of surface morphology on atmospheric corrosion behaviour of Fe-based metallic glass Fe₆₇Co₁₈Si₁₄. *Bull Mater Sci*. 2008;31(4):693–698. doi: 10.1007/s12034-008-0110-5.
39. Wu KH, Chao CM, Yeh TF, Chang TC. Thermal stability and corrosion resistance of polysiloxane coatings on 2024-T3 and 6061-T6 aluminum alloy. *Surf Coat Technol*. 2007;201(12):5782–5788. doi: 10.1016/j.surfcoat.2006.10.024.
40. Guo XH. Effect of sol composition on corrosion protection of SNAP film coated on magnesium alloy. *Chin J Inorg Chem*. 2009;25(7):1254–1261.
41. Singh RK, Bihari B, Alam N. Study of corrosion ferrous and non-ferrous in aqueous medium. *Int J Metall Alloy*. 2025;11(1):44–50. doi: 10.37628/IJMA.
42. Singh RK, Ayush M, Singh JP. Corrosion and corrosion protection of cast iron due to bio-organism. *J Mod Chem Chem Technol*. 2025;16(2):105–114. doi: 10.37591/JoMCCT.